International Journal of Chemistry; Vol. 5, No. 3; 2013
ISSN 1916-9698 E-ISSN 1916-9701
Published by Canadian Center of Science and Education

Phase Transition and Crystal Structure of $CsHSeO_4$ and $CsDSeO_4$ Crystals

Takanori Fukami[1], Shuta Tahara[1], Keiko Nakasone[1] & Mitsuhiro Seino[1]

[1] Department of Physics and Earth Sciences, Faculty of Science, University of the Ryukyus, Japan

Correspondence: Takanori Fukami, Department of Physics and Earth Sciences, Faculty of Science, University of the Ryukyus, Okinawa 903-0213, Japan. Tel: 81-98-895-8509. E-mail: fukami@sci.u-ryukyu.ac.jp

Received: April 10, 2013 Accepted: May 17, 2013 Online Published: May 29, 2013

doi:10.5539/ijc.v5n3p1 URL: http://dx.doi.org/10.5539/ijc.v5n3p1

Abstract

DSC, TG-DTA and X-ray diffraction measurements have been performed on cesium hydrogen selenate $CsHSeO_4$ and deuterated $CsDSeO_4$ crystals. The superionic phase transitions for the proton and deuterated compounds were found to occur at 402.6 and 398.1 K, respectively. The thermal decomposition accompanied by hydrolysis in both compounds started at around the transition temperature, and the maximum rate of weight loss from the reaction was observed at around 490 K. The space group symmetry (monoclinic $P2_1/c$) and structural parameters were determined at 298 and 355 K. The expansion of the O-H-O hydrogen bond at room temperature by the substitution of deuterium for hydrogen was observed to be 0.015(7) Å. The geometric isotope effect on the hydrogen bond structure by deuteration was realized in the $CsHSeO_4$ crystal. The experimental results denied the existence of a phase transition from phase II to III in the proton and deuterated compounds.

Keywords: $CsHSeO_4$, $CsDSeO_4$, crystal structure, phase transition, isotope effect, DSC, TG-DTA, X-ray diffraction

1. Introduction

Alkali (or ammonium) ions ($M^+ = K^+$, Rb^+, Cs^+, or NH_4^+) and sulfate (or selenate) ions (XO_4^{2-}, where X = S or Se) exist generally in five types of compounds with the following chemical formulas: M_2XO_4, $MHXO_4$, $M_3H(XO_4)_2$, $M_5H_3(XO_4)_4$, and $M_3H_5(XO_4)_4$. Many crystals of these types are superionic conductors at high temperature. Some of them are characterized by their isomorphism, ferroelasticity, ferroelectricity and sequential structural phase transitions. The physical properties and phase transition mechanisms for these types have been widely studied by using many experimental methods.

Cesium hydrogen selenate ($CsHSeO_4$) crystal belongs to a family of $MHXO_4$-type compounds, and undergoes two phase transitions at $T_{I\text{-}II}$ (401 K) and $T_{II\text{-}III}$ (323-370 K) with three phases (Baranov et al., 1982, 1984; Checa et al., 2009; Colomban et al., 1986; Kamazawa et al., 2010; Komukae et al., 1990; Luspin et al., 1995, 2000; Ortiz et al., 2008; Pham-Thi et al., 1985; Yokota, 1982; Yokota et al., 1982). These phases are denoted as I, II, and III in order of decreasing temperature. The crystal is a superionic conductor in phase I and ferroelastic in phase III (Baranov et al., 1982, 1984; Komukae et al., 1990; Yokota, 1982; Yokota et al., 1982). The structure at room temperature has been found to be monoclinic with space group $P2_1/c$ containing four molecules in the unit cell with lattice parameters a = 7.978(1), b = 8.420(1), c = 7.813(1) Å, and β = 111.34(1)º, and to consist of a one-dimensional hydrogen bonded zigzag chain along the c-axis (Baran & Lis, 1987; Komukae et al., 1990). The bond length of the O-H-O hydrogen bond connecting SeO_4 tetrahedra is 2.603(15) Å. Moreover, the structure in phase I has been reported to be tetragonal with space group $I4_1/amd$ (Foose & Mitra, 1977; Komukae et al., 1990; Yokota, 1982).

The transition temperature $T_{I\text{-}II}$ in all published papers for the $CsHSeO_4$ crystal is very close to 401 K, almost without exception. However, the transition temperature $T_{II\text{-}III}$ is in the range of 323–370 K depending on the type of investigation (Baranov et al., 1982; Checa et al., 2009; Colomban et al., 1986; Luspin et al., 1995, 2000; Ortiz et al., 2008; Pham-Thi et al., 1985). The reason for the wide spread of $T_{II\text{-}III}$ is most likely to be due to sample quality. For example, three endothermic peaks in DSC curves have been described in the previous paper by Ortiz et al. (2008), despite that the presence of either one or two transitions has already been reported in many papers. This anomaly is inferred to be caused by using low-quality samples in their experiments, and this type of mistake can be eliminated by inspecting the crystal structure of sample. By removing obviously deviant data the phase transition temperature $T_{II\text{-}III}$ from phase II to III can be modified to be in the range of 323–350 K (Checa et al.,

2009; Colomban et al., 1986; Luspin et al., 1995, 2000; Pham-Thi et al., 1985).

In contrast to $CsHSeO_4$ crystal, studies on deuterated cesium hydrogen selenate ($CsDSeO_4$) crystal are extremely rare. The velocity of sound and the elastic constants for the deuterated crystal have been obtained at 293 K, and the space groups in room- and high-temperature phases have been determined to be monoclinic $P2_1/c$ and tetragonal $I4_1/amd$, respectively (Balagurov et al., 1986; Lushnikov et al., 1987). Moreover, structural information on partially deuterated crystal with deuteration level x = 70% has been obtained at room temperature by analyzing neutron powder diffraction data using the Rietveld method (Balagurov et al., 1987). However, the accurate crystal structure of $CsDSeO_4$ and the isotope effect on properties of $CsHSeO_4$ by substitution of deuterium for hydrogen have not yet been reported.

The purpose of this paper is to report the phase transition from phase II to III in $CsHSeO_4$ and $CsDSeO_4$ crystals, and to determine the crystal structure of the room-temperature phase of $CsDSeO_4$. Isotope effects on the structure and properties of the $CsHSeO_4$ crystal by deuteration have been studied.

Table 1. Crystal data, intensity collections and structure refinements for $CsHSeO_4$ and $CsDSeO_4$ at 298 and 355K

Compound	$CsHSeO_4$		$CsDSeO_4$	
M_r	276.88		277.88	
Crystal color	Colorless		Colorless	
Temperature [K]	298	355	298	355
Crystal system	Monoclinic	Monoclinic	Monoclinic	Monoclinic
Space group	$P2_1/c$	$P2_1/c$	$P2_1/c$	$P2_1/c$
a [Å]	7.9988(7)	8.0208(6)	7.9972(6)	8.0228(7)
b [Å]	8.4360(6)	8.4424(5)	8.4314(5)	8.4397(6)
c [Å]	7.8264(7)	7.8530(7)	7.8295(8)	7.8569(9)
β [º]	111.303(3)	111.463(3)	111.407(3)	111.557(3)
V [Å^3], Z	492.02(7), 4	494.89(6), 4	491.50(7), 4	494.78(8), 4
D(cal.) [Mg/m^3], μ(Mo K_α)	3.738, 14.817	3.716, 14.731	3.755, 14.833	3.730, 14.735
Sample shape	Sphere	Sphere	Sphere	Sphere
Size in diameter 2r [mm]	0.30	0.30	0.34	0.34
θ range [º]	3.65-37.57	2.73-37.83	3.65-37.84	2.73-37.68
Index ranges	$-13\le h\le 13$	$-13\le h\le 13$	$-13\le h\le 13$	$-13\le h\le 13$
	$-14\le k\le 14$	$-14\le k\le 14$	$-14\le k\le 14$	$-14\le k\le 14$
	$-13\le l\le 13$	$-13\le l\le 13$	$-13\le l\le 13$	$-13\le l\le 13$
Reflections collected, unique	13523, 2567	13661, 2602	13577, 2575	13638, 2585
R(int)	0.0469	0.0446	0.0946	0.0574
Completeness to θ [%]	98.7	97.8	97.2	98.0
Absorption correction type	Spherical	Spherical	Spherical	Spherical
Transmission factor T_{min}-T_{max}	0.0579-0.0979	0.0579-0.0984	0.0425-0.0816	0.0425-0.0814
Date [$I>2\sigma(I)$], parameters	1859, 60	1768, 60	1521, 60	1669, 60
R_1, wR_2 (final indices)	0.0292, 0.0760	0.0318, 0.0819	0.0309, 0.0941	0.0286, 0.0878
R_1, wR_2 (all data)	0.0496, 0.0820	0.0601, 0.0922	0.0553, 0.0978	0.0610, 0.0974
Factors a and b in weighting*	0.0291, 0.0424	0.0323, 0.3974	0.0209, 0.0	0.0315, 0.0519
Goodness-of-fit on F^2	1.206	1.146	1.017	1.172
Extinction coefficient	0.0390(12)	0.0245(9)	0.0207(8)	0.0143(8)
Largest diff. peak and hole	1.855, -0.711	1.114, -1.069	2.089, -1.686	0.739, -1.089

*Weighting scheme: $w=1/[\sigma^2(F_o^2)+(aP)^2+bP]$, $P=(F_o^2+2F_c^2)/3$.

2. Experimental

2.1 Crystal Growth

Single crystals of $CsHSeO_4$ and $CsDSeO_4$ were grown at room temperature by slow evaporation from aqueous solutions containing a molar ratio 1:2 of Cs_2CO_3 and H_2SeO_4 in desiccators over P_2O_5. The deuterated crystals thus obtained were recrystallized five times from a mixed D_2O solution by the evaporation method. The grown crystals had platelike shapes.

2.2 Thermal Measurements

Differential scanning calorimetry (DSC) and thermogravimetric-differential thermal analysis (TG-DTA) measurements were carried out in the temperature range of 100-600 K using DSC7020 and TG/DTA7300 systems from Seiko Instruments Inc, respectively. The sample amounts for the DSC and TG-DTA measurements varied between 3.28 and 10.97 mg, and the heating and cooling rates were 5 or 10 K/min with flowing dry N_2 gas.

2.3 X-Ray Crystal Structure Determination

The X-ray diffraction measurements were carried out at 298 (phase III) and 355 (phase II) K on a Rigaku Saturn CCD X-ray diffractometer with graphite monochromated Mo K_α radiation (λ = 0.71073 Å). Diffraction data were collected by using an ω scan mode with a detector distance of 40 mm to the sample crystal, and the data were processed using the CrystalClear software package. Intensity data were corrected for Lorentz polarization and absorption effects. The structures were solved with direct methods of SIR2008 and refined on F^2 by full-matrix least-squares methods using the SHELXL-97 program in the WinGX program package (Burla et al., 2007; Farrugia, 1999; Scheldrick, 1997). A summary of crystal data, intensity data collections, and structure refinements is given in Table 1.

3. Results and Discussion

3.1 Thermal Analysis

Figure 1 shows the DSC curves of (a) $CsHSeO_4$ and (b) $CsDSeO_4$ crystals for heating and cooling in the temperature range from room temperature to 455 K. The endothermic and exothermic peaks in the DSC curves respectively are clearly seen at 403.6 and 390.7 K for the proton compound, and at 399.3 and 384.8 K for the deuterated compound. The temperature hysteresis between the endothermic and exothermic peak temperatures in both compounds is about 14 K. Moreover, there are slight decreases in the DSC peak temperature between the two compounds. The decreases in the peak temperature of the heating and cooling curves by deuteration are about 4 and 6 K, respectively. The decrease of the DSC peak temperature can also be seen in the previously reported papers of $Na_3H(SO_4)_2$ and $(NH_4)_3H(SeO_4)_2$ crystals (Fukami & Chen, 1999, 2003). The onset temperatures of the endothermic and exothermic peaks are respectively determined to be 402.6 and 392.0 K for the proton compound, and 398.1 and 385.6 K for the deuterated compound. The onset temperature in the heating curve for the proton compound is very close to the I-II transition temperature (401 K) (Kamazawa et al., 2010; Komukae et al., 1990; Luspin et al., 1995, 2000; Yokota et al., 1982). Generally, it is believed that a clear peak in the DSC chart is attributed to the change of exchange energy at phase transition in almost all cases. A first-order phase transition is characterized by a sharp endothermic peak at transition and is accompanied by a thermal hysteresis with transition temperature. Therefore, we concluded that the proton and deuterated crystals undergo a first-order structural phase transition at 402.6 and 398.1 K, respectively. However, the DSC peak corresponding to the II-III phase transition previously reported by some investigators can not be seen in the curves for both compounds, as shown in Figure 1. Moreover, no significant endothermic or exothermic peaks in DSC curves were observed in the temperature range of 100 K to room temperature. Therefore, these results indicate that there is no phase transition in the temperature range of 100–400 K for both compounds.

The transition enthalpies ΔH (entropies ΔS) obtained from the endothermic and exothermic peaks are respectively determined to be 6.26 (1.87R) and 5.84 kJ mol^{-1} (1.79R) for the proton compound, and 6.11 (1.85R) and 5.39 kJ mol^{-1} (1.68R) for the deuterated compound, where R is the gas constant (8.314 $JK^{-1}mol^{-1}$). The obtained ΔH (or ΔS) for both compounds is very close to the reported values of 5.74 kJ mol^{-1} and 1.94R (Friesel et al., 1989; Yokota et al., 1982). Table 2 shows the peak temperatures, transition temperatures T_c (onset temperatures), transition enthalpies ΔH and entropies ΔS determined from the DSC curves of the proton and deuterated compounds.

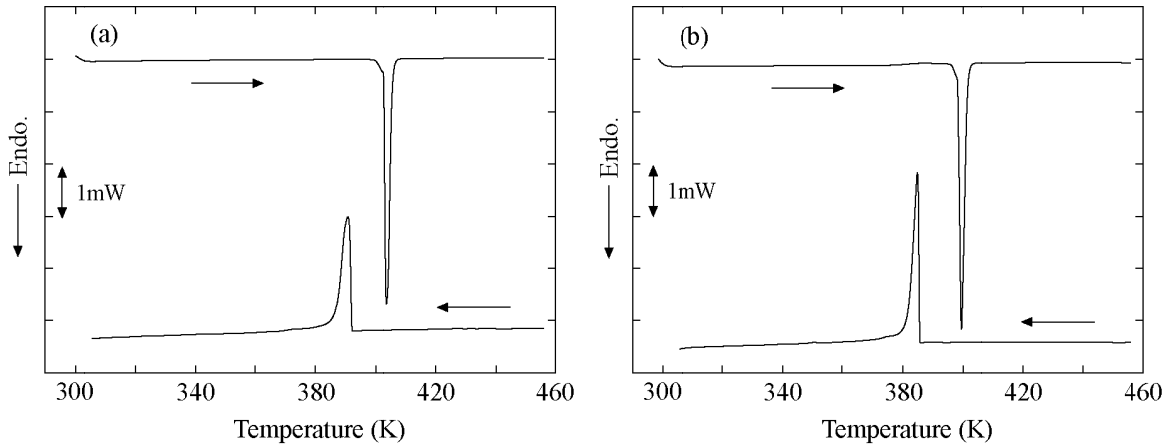

Figure 1. DSC curves for heating and cooling of (a) $CsHSeO_4$ and (b) $CsDSeO_4$. Sample weights of $CsHSeO_4$ and $CsDSeO_4$ were 4.94 and 5.43 mg, respectively. The heating and cooling rates were 5 K/min under a dry nitrogen flux of 40 ml/min

Table 2. Peak temperatures, transition temperatures T_c (onset temperatures), transition enthalpies ΔH and entropies ΔS obtained from (a) DSC, (b) DTA and (c) DTG curves for $CsHSeO_4$ and $CsDSeO_4$

		$CsHSeO_4$					$CsDSeO_4$				
		heating				cooling	heating				cooling
(a) DSC	Peak temp. [K]	403.6				390.7	399.3				384.8
	T_c [K]	402.6				392.0	398.1				385.6
	ΔH [kJ mol^{-1}]	6.26				5.84	6.11				5.39
	$\Delta S/R$	1.87				1.79	1.85				1.68
(b) DTA	Peak temp. [K]	406.5	487.9	518.0	540.7		405.2	487.5	518.1	541.3	
	T_c [K]	401.4					399.8				
(c) DTG	Peak temp. [K]		485.4					486.1			

Gas constant R=8.314 JK^{-1}mol^{-1}.

Figure 2 shows the TG, differential TG (DTG), and DTA thermal analysis curves for $CsHSeO_4$ and $CsDSeO_4$ at temperatures up to 600 K. The two distinct and two weak endothermic peaks are seen in the DTA curves for both compounds, and a large peak is also seen in the DTG curves. The peak and onset temperatures in the DTA curves are respectively determined to be 406.5 and 401.4 K for the proton compound, and 405.2 and 399.8 K for the deuterated compound. The sharp peak at around 400 K in the DTA curves corresponds to the superionic transition. The onset temperatures for both compounds are very close to those obtained from the DSC curves. Large peaks in the DTG curves for the proton and deuterated compounds respectively are seen at 485.4 and 486.1 K, and these correspond to the large endothermic peak at about 488 K in the DTA curves. The peak and onset temperatures determined from the DTA and DTG curves are listed in Table 2. The differences in the peak and onset temperatures between the proton and deuterated compounds are about 1 and 2 K, respectively. Apparent slight decreases in the peak and onset temperatures by deuteration are observed, and these are similar to the results from the DSC curves.

The TG and DTG curves exhibit a weight loss owing to the decomposition process of sample. The large peak at 488 K in the DTA curves is mainly attributed to the thermal decomposition of the sample. Moreover, a slight deviation from the baseline in the TG curves for both compounds can be seen at around the superionic transition temperature. This indicates that the thermal decomposition reaction of the sample starts at around the transition temperature. The weight loss at around 490 K obtained from the TG curves for the proton and deuterated compounds is 3.31 and 3.43%, respectively. Similarly to the thermal decomposition of $CsHSO_4$ (Ortiz et al., 2006, 2008), we assume a reaction in which two molecules of $CsH(D)SeO_4$ typically dissolve to $Cs_2Se_2O_7$ and $H(D)_2O$ as follows:

$$2\ CsH(D)SeO_4 \rightarrow Cs_2Se_2O_7 + H(D)_2O.$$

Since the weight loss is accompanied by the evolution of $H(D)_2O$ molecules, the theoretical weight loss for the proton and deuterated compounds is calculated to be 3.25% [=18.02/(2×276.88)] and 3.60% [= 20.03/(2×277.88)], respectively. These values are very close to the experimental weight losses of 3.31 and 3.43%, respectively. Thus, it is concluded that the weight loss at around 490 K is caused by the evaporation of $H(D)_2O$ vapor from the decomposition of the sample. The two weak peaks at about 518 and 541 K in the DTA curves for both compounds are presumed to be associated with the behavior of thermal properties of $Cs_2Se_2O_7$. Similarly to the results obtained by DSC, no peak corresponding to the II-III transition is observed in the DTA, TG and DTG curves for both compounds.

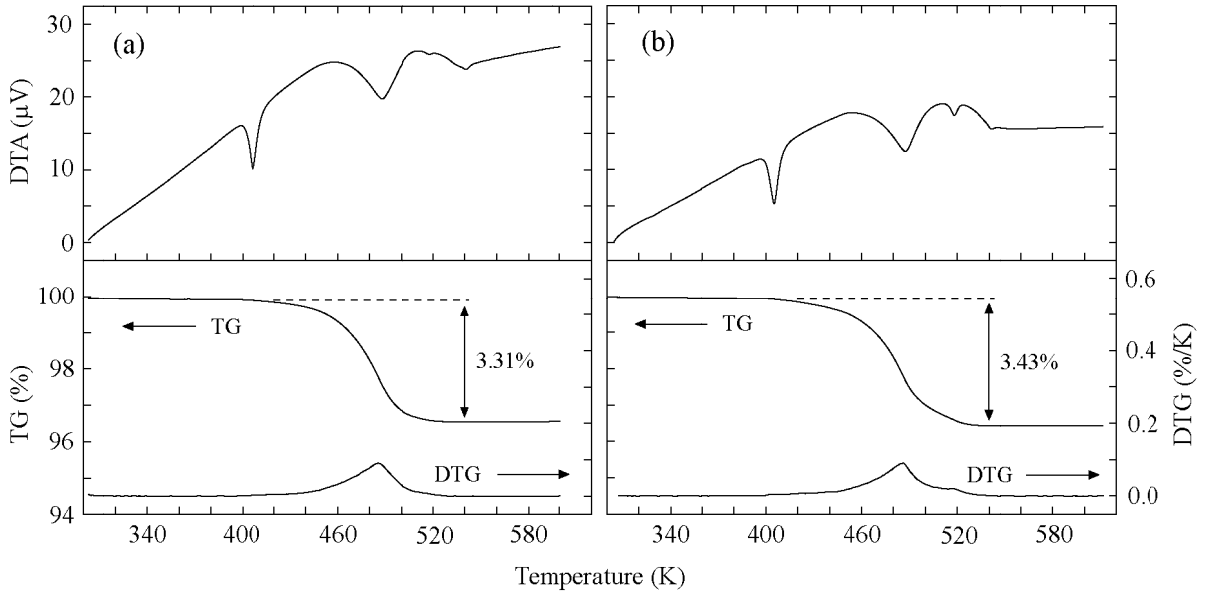

Figure 2. TG, DTG, and DTA thermograms for (a) $CsHSeO_4$ and (b) $CsDSeO_4$ for heating. Sample weights (powder) of $CsHSeO_4$ and $CsDSeO_4$ were 8.22 and 8.10 mg, respectively. The heating rate was 10 K/min under a dry nitrogen flux of 300 ml/min

3.2 X-Ray Crystal Structure Description

In $CsHSeO_4$ and $CsDSeO_4$, the crystal structures at 298 (phase III) and 355 K (phase II) were analyzed by X-ray diffraction. The lattice parameters calculated from all reflections indicated that they belong to monoclinic system. The systematic extinctions of the reflections revealed that the space groups are determined to be $P2_1/c$. Moreover, weak reflections owing to superlattice structure were observed in many samples for both compounds, as similarly reported by Komukae et al. (1990). The *R* factor calculated for the reflections observed from these samples in the refinement was not reduced to below 4 %. Thus, in order to obtain accurate structural information, we carefully chose samples for which the diffraction pattern showed no superlattice reflections. As a result, as shown in Table 1, the *R* factor and the highest peak of residual electron density in the final difference Fourier map were calculated to be around 3 % and below 2.1 e $Å^{-3}$, respectively.

Figure 3 shows perspective views of (a) $CsHSeO_4$ and (b) $CsDSeO_4$ structures on the *ac*-plane at room temperature. The positional parameters in fractions of a unit cell and the thermal parameters are listed in Table 3. The selected bond lengths (in Å) and angles (in degrees) are given in Table 4. The hydrogen bond geometry (in Å and degrees) is presented in Table 5.

Table 3. Atomic coordinates and thermal parameters ($\times 10^4$Å^2) at 298 and 355 K for (a) $CsHSeO_4$ and (b) $CsDSeO_4$ with standard deviations in brackets. The anisotropic thermal parameters are defined as $\exp[-2\pi^2(U_{11}a^{*2}h^2+U_{22}b^{*2}k^2+U_{33}c^{*2}l^2+2U_{23}b^*c^*kl+2U_{13}a^*c^*hl+2U_{12}a^*b^*hk)]$. Isotropic thermal parameters (Å^2) for H(D) atoms are listed under U_{11}

(a) $CsHSeO_4$

Temp.	Atom	x	Y	z	U_{11}	U_{22}	U_{33}	U_{23}	U_{13}	U_{12}
298 [K]	Cs	0.78992(3)	0.12819(3)	0.29379(3)	274(1)	304(1)	283(1)	-10.0(9)	88.3(8)	-18.5(8)
	Se	0.25403(5)	0.12609(4)	0.22086(5)	234(2)	208(2)	232(2)	10(1)	94(1)	13(1)
	O(1)	0.4309(4)	0.2178(4)	0.3859(5)	264(14)	601(21)	531(20)	-288(17)	99(14)	-21(13)
	O(2)	0.1031(4)	0.2584(4)	0.1351(4)	377(16)	413(16)	440(17)	61(13)	80(14)	174(13)
	O(3)	0.1880(5)	-0.0180(3)	0.3137(5)	651(23)	336(16)	590(21)	105(14)	414(19)	-36(14)
	O(4)	0.3490(4)	0.0658(3)	0.0803(4)	461(17)	364(15)	336(14)	0(12)	245(13)	63(13)
	H	0.442(9)	0.267(7)	0.476(8)	0.09(2)					
355 [K]	Cs	0.78850(4)	0.12793(3)	0.29374(4)	346(1)	378(2)	351(1)	-12(1)	112.2(9)	-22(1)
	Se	0.25272(5)	0.12557(4)	0.22002(5)	299(2)	263(2)	289(2)	13(1)	123(1)	16(1)
	O(1)	0.4290(5)	0.2182(5)	0.3853(6)	339(17)	754(26)	635(24)	-328(21)	109(16)	-8(16)
	O(2)	0.1021(5)	0.2575(4)	0.1353(5)	461(20)	546(21)	530(21)	81(16)	99(16)	214(16)
	O(3)	0.1870(6)	-0.0177(4)	0.3125(6)	807(28)	421(19)	717(27)	120(17)	494(23)	-46(18)
	O(4)	0.3477(5)	0.0666(4)	0.0803(5)	576(21)	497(18)	422(18)	1(15)	301(16)	83(16)
	H	0.418(9)	0.262(8)	0.486(9)	0.08(2)					

(b) $CsDSeO_4$

Temp.	Atom	x	Y	z	U_{11}	U_{22}	U_{33}	U_{23}	U_{13}	U_{12}
298 [K]	Cs	0.78970(4)	0.12812(4)	0.29348(4)	267(2)	303(2)	294(2)	-8(1)	97(1)	-17(1)
	Se	0.25350(6)	0.12563(5)	0.22043(6)	226(2)	212(2)	237(2)	9(2)	99(2)	15(2)
	O(1)	0.4309(5)	0.2171(6)	0.3842(7)	254(19)	548(28)	591(30)	-239(24)	120(18)	-23(17)
	O(2)	0.1041(5)	0.2582(5)	0.1358(5)	386(21)	394(23)	445(23)	48(17)	106(17)	164(17)
	O(3)	0.1865(6)	-0.0177(4)	0.3132(6)	679(28)	290(21)	588(28)	73(18)	419(22)	-61(19)
	O(4)	0.3485(5)	0.0659(5)	0.0804(5)	466(22)	406(22)	353(20)	-5(17)	269(17)	51(17)
	D	0.442(10)	0.258(10)	0.463(10)	0.08(3)					
355 [K]	Cs	0.78824(4)	0.12785(3)	0.29349(4)	318(2)	388(2)	374(2)	-10(1)	107(1)	-21(1)
	Se	0.25228(5)	0.12499(4)	0.21987(5)	272(2)	276(2)	308(2)	11(2)	116(1)	16(1)
	O(1)	0.4291(5)	0.2182(5)	0.3856(6)	306(17)	697(24)	720(26)	-302(21)	125(16)	-13(16)
	O(2)	0.1024(5)	0.2575(4)	0.1341(5)	457(21)	525(22)	601(23)	65(16)	102(17)	210(16)
	O(3)	0.1857(6)	-0.0183(4)	0.3118(6)	832(30)	420(19)	763(28)	104(18)	521(24)	-68(18)
	O(4)	0.3475(5)	0.0664(4)	0.0810(5)	512(21)	508(19)	486(19)	-4(16)	296(16)	72(16)
	D	0.417(9)	0.266(8)	0.504(9)	0.09(2)					

The observed crystal structures for both compounds at 298 and 355 K are very close to the previously determined structure of $CsHSeO_4$, and consist of O-H(D)-O hydrogen bonds connecting adjacent SeO_4 tetrahedra, forming a one-dimensional zigzag chain along the *c*-axis (Baran & Lis, 1987; Komukae et al., 1990). The bond length of the O-H-O hydrogen bond at 298 and 355 K has the same value of 2.608(5) Å. However, the length of the O-D-O hydrogen bond decreases from 2.623(6) to 2.613(5) Å with increasing temperature. This implies that the O atoms of the O-D-O hydrogen bond are slightly displaced into a more stable position with increasing temperature. In all the observed structures, the SeO_4 tetrahedra are slightly disorder from a regular tetrahedron because the magnitudes of the O(1)-O(4) length and O(1)-Se-O(4) angle differ from those of the

other lengths and angles in the SeO_4 tetrahedra, respectively. Moreover, the two bond distances between the Se atom and the O atoms (O(1) and O(4)) ended to the H(D) atom (the distance of the Se-O(-H(D)) bond) are longer than that of the other Se-O bonds. These characteristics of bond length and angle can be seen in all the four structures, and the magnitudes in these differences are almost the same value. Thus, it is considered that there exists a bonding strength between the O atoms involved in the O(1)-H(D)-O(4) hydrogen bond, and the bonding strength is not affected by deuteration. The bonding strength has also been reported in previous papers on $Na_3H(SO_4)_2$ and $(NH_4)_3H(SeO_4)_2$ crystals (Fukami & Chen, 1999, 2003).

Table 4. Selected interatomic distances (in Å) and angles (in degrees) for (a) $CsHSeO_4$ and (b) $CsDSeO_4$ at 298 and 355 K

	(a) $CsHSeO_4$		(b) $CsDSeO_4$	
Temp.	298 [K]	355 [K]	298 [K]	355 [K]
Cs-O(2)[(a)]	3.076(3)	3.085(3)	3.083(3)	3.081(3)
Cs-O(3)[(b)]	3.123(3)	3.131(4)	3.125(4)	3.127(4)
Cs-O(3)[(c)]	3.152(3)	3.166(4)	3.156(4)	3.169(4)
Cs-O(4)[(d)]	3.181(3)	3.189(3)	3.179(4)	3.190(3)
Cs-O(2)[(e)]	3.229(3)	3.241(4)	3.227(4)	3.240(4)
Cs-O(1)	3.292(3)	3.306(4)	3.284(4)	3.308(4)
Cs-O(4)	3.351(3)	3.353(4)	3.348(4)	3.350(4)
Cs-O(2)[(f)]	3.359(3)	3.371(4)	3.354(5)	3.372(4)
Cs-O(3)[(f)]	3.365(4)	3.377(4)	3.364(4)	3.382(4)
Se-O(1)	1.715(3)	1.718(4)	1.710(4)	1.723(4)
Se-O(2)	1.602(3)	1.598(3)	1.594(3)	1.599(3)
Se-O(3)	1.601(3)	1.597(3)	1.600(4)	1.598(3)
Se-O(4)	1.629(3)	1.626(3)	1.625(4)	1.622(3)
O(1)-O(2)	2.666(4)	2.660(5)	2.650(6)	2.661(5)
O(1)-O(3)	2.693(5)	2.692(6)	2.694(6)	2.702(5)
O(1)-O(4)	2.580(4)	2.580(5)	2.563(6)	2.578(5)
O(2)-O(3)	2.677(4)	2.665(5)	2.666(5)	2.670(5)
O(2)-O(4)	2.703(4)	2.699(5)	2.694(5)	2.691(5)
O(3)-O(4)	2.684(4)	2.686(5)	2.687(5)	2.686(5)
O(1)-O(4)[(b)]	3.384(4)	3.403(5)	3.388(6)	3.402(5)
O(2)-O(3)[(g)]	3.133(4)	3.137(5)	3.131(5)	3.135(5)
O(4)-O(4)[(d)]	3.295(5)	3.329(6)	3.304(7)	3.340(6)
O(1)-Se-O(2)	106.9(2)	106.6(2)	106.6(2)	106.4(2)
O(1)-Se-O(3)	108.6(2)	108.6(2)	108.9(3)	108.9(2)
O(1)-Se-O(4)	101.0(2)	100.9(2)	100.4(2)	100.8(2)
O(2)-Se-O(3)	113.4(2)	113.1(2)	113.2(2)	113.3(2)
O(2)-Se-O(4)	113.6(2)	113.7(2)	113.7(2)	113.4(2)
O(3)-Se-O(4)	112.4(2)	112.9(2)	112.9(2)	113.1(2)

Symmetry codes: (a) x+1,-y+1/2,z+1/2; (b) -x+1,y+1/2,-z+1/2; (c) -x+1,-y,-z+1; (d) -x+1,-y,-z; (e) -x+1,y-1/2,-z+1/2; (f) x+1,y,z; (g) -x, y-1/2, -z+1/2.

Except for the O(1)-H(D)-O(4) hydrogen bond, there are three O-O bonds (O(1)-O(4), (2)-O(3) and O(4)-O(4)) between two adjacent SeO_4 tetrahedra in all the observed structures, as shown in Table 4. For example, the

lengths of the O(1)-O(4), (2)-O(3) and O(4)-O(4) bonds in the proton compound at 298 K are 3.384(4), 3.133(4) and 3.295(5) Å, respectively. The remaining peak in the difference Fourier synthesis during structure refinement is found at around the center in the three O-O bonds. Therefore, it is possible that a hydrogen atom is located almost at the center of these O-O bonds. Based on NMR results, Yoshida et al. have suggested that all protons in $CsHSeO_4$ move to interstitial sites with broken hydrogen bonds in the temperature range of 370-401 K, and the proton in hydrogen bonds and the moving proton with the broken one coexist in the range of 160-370 K (Yoshida et al., 2005, 2008). Therefore, it is considered that the protons below the transition temperature (402.6 K) may transfer between four positions (one noncenter and three center positions) in the O-H-O hydrogen and three O-O bonds.

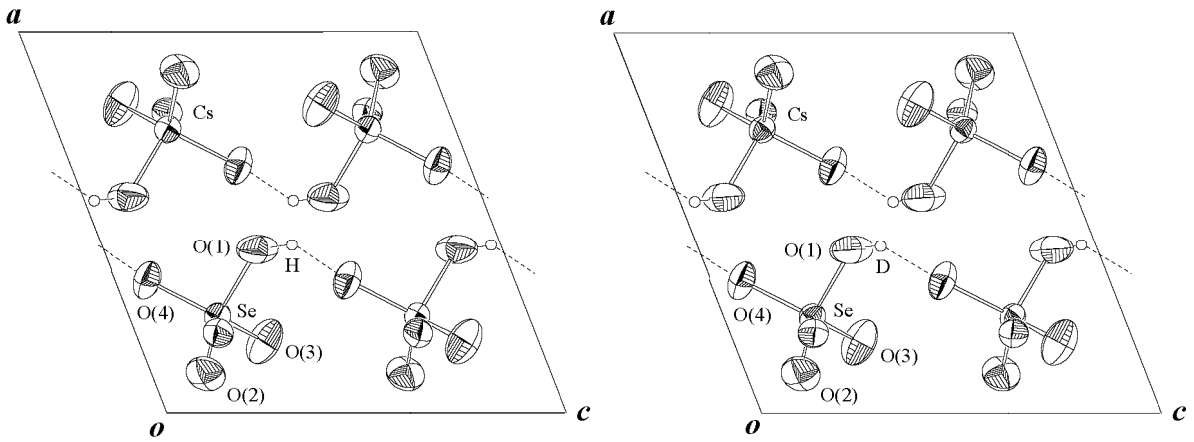

Figure 3. Perspective views of (a) $CsHSeO_4$ and $CsDSeO_4$ structures on the *ac*-plane at 298 K with 60% probability-displacement thermal ellipsoids. The dashed lines show O-H(D)-O hydrogen bonds

Table 5. Hydrogen bond distances (in Å) and angles (in degrees) for (a) $CsHSeO_4$ and (b) $CsDSeO_4$ at 298 and 355 K

	Temp.	O(1)-H(D)	H(D)···O(4)[(a)]	O(1)···O(4)[(a)]	OH(D)O[(a)]
(a) $CsHSeO_4$	298 [K]	0.80(6)	1.91(6)	2.608(4)	146(7)
	355 [K]	0.91(6)	1.81(6)	2.608(5)	146(6)
(b) $CsDSeO_4$	298 [K]	0.68(7)	2.03(8)	2.623(6)	146(8)
	355 [K]	1.05(7)	1.71(7)	2.613(5)	141(5)

Symmetry codes: (a) $x,-y+1/2,z+1/2$.

3.3 Phase Transition from Phase II to III

As described in the Introduction, the II-III phase transition temperature is in the range of 323–350 K except for that obtained from poor-quality samples. Differences in crystal symmetry and structural parameters at temperatures between 298 and 355 K could not be found in both compounds. Moreover, no peak corresponding to the II-III transition was observed in the DSC, TG, DTG and DTA thermogram curves. Thus, we conclude that the II-III phase transition (that is, phase II) does not exist in $CsHSeO_4$ and $CsDSeO_4$ crystals.

3.4 Geometric Isotope Effect

Ichikawa has pointed out the geometric isotope effect on O-H-O hydrogen bond structure, based on many accurate data concerning the crystal structures and related properties of O-H-O hydrogen-bonded crystals (Ichikawa, 1978, 2000). The expansion of the bond length upon deuteration is reported as the length varied in the range of about 2.43 to 2.65 Å, and the maximum magnitude of the expansion is about 0.03 Å at a length of around 2.5 Å. Figure 4 shows the expansion ΔR of the O-H-O hydrogen bond upon deuteration as a function of the hydrogen bond length (Ichikawa, 1978, 2000; Fukami et al., 2010a, 2010b). The bond length (2.608(4) Å) of

the O-H-O hydrogen bond in $CsHSeO_4$ is in the range of the expansion, as shown in Table 5. The expansions of the bond length at 298 and 355 K upon deuteration are observed to be 0.015(7) and 0.005(7) Å, respectively. The value of 0.015(7) Å is added in Figure 4, and it is in good agreement with the data for the expansions of other compounds. Thus, the geometric isotope effect on the O-H-O hydrogen bond structure at room temperature is realized in the $CsHSeO_4$ crystal.

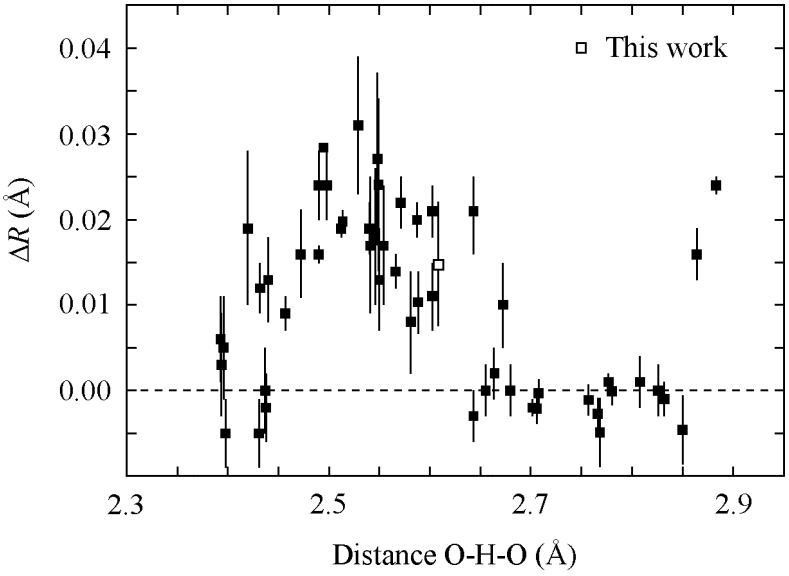

Figure 4. Expansions ΔR [$=d_{(O\text{-}D\text{-}O)} - d_{(O\text{-}H\text{-}O)}$] of O-H-O hydrogen bonds upon deuteration as a function of hydrogen bond distance (Ichikawa, 1978, 2000; Fukami et al., 2010a, 2010b)

4. Conclusion

We summarize the results from DSC, TG-DTA and X-ray diffraction measurements for $CsHSeO_4$ and $CsDSeO_4$ crystals. The superionic phase transition temperatures for the proton and deuterated compounds are found to be 402.6 and 398.1 K, respectively. Moreover, it is found that the thermal decomposition for both compounds starts at around the transition temperature, and the maximum rate of weight loss takes place at around 490 K. We suggest that the weight loss of the samples is attributed to the evaporation of $H(D)_2O$ vapor formed by reaction with $Cs_2Se_2O_7$. The crystal structures of the proton and deuterated compounds at 298 and 355 K are determined to be monoclinic with space group $P2_1/c$ by means of single-crystal X-ray diffraction. The results obtained from three different types of measurements indicate no structural phase transition from phase II to III in the proton and deuterated compounds, and those from DSC and TG-DTA also indicate that there is no phase transition in the temperature range of 100–400 K. The expansion of the O-H-O hydrogen bond at room temperature by the substitution of deuterium for hydrogen is observed to be 0.015(7) Å. The geometric isotope effect on the O-H-O hydrogen bond structure by deuteration is confirmed to exist in the $CsHSeO_4$ crystal.

References

Balagurov, A. M., Beskrovnyi, A. I., Datt, I. D., Shuvalov, L. A., & Shchagina, N. M. (1986). Neutron-diffraction investigation of superionic phase transition in cesium hydro-and deuteroselenates. *Sov. Phys. Crystallogr., 31*, 643-647.

Balagurov, A. M., Beskrovnyi, A. I., Savenko, B. N., Merinov, B. V., Dlouhá, M., Vratislav, S., & Jirák, Z. (1987). The room temperature structure of deuterated $CsHSO_4$ and $CsHSeO_4$. *Phys. Stat. Sol. (a), 100*(1), K3-K7. http://dx.doi.org/10.1002/pssa.2211000146

Baran, J., & Lis, T. (1987). Structure of caesium hydrogenselenate. *Acta Crystallogr. C, 43*(5), 811-813. http://dx.doi.org/10.1107/S0108270187093971

Baranov, A. I., Fedosyuk, R. M., Schagina, N. M., & Shuvalov, L. A. (1984). Structural phase transitions to the state with anomalously high-ionic conductivity in some perroelectric and ferroelastic crystals of the bisulpate group. *Ferroelectrics Lett., 2*(1), 25-28. http://dx.doi.org/10.1080/07315178408202428

Baranov, A. I., Shuvalov, L. A., & Shchagina, N. M. (1982). Superion conductivity and phase transitions in $CsHSO_4$ and $CsHSeO_4$ crystals. *JETP Lett., 36*(11), 459-462. Retrieved from http://www.jetpletters.ac.ru/ps/1339/article_20210.pdf

Burla, M. C., Caliandro, R., Camalli, M., Carrozzini, B., Cascarano, G. L., Caro, L. D., ... Spagna, R. (2007). IL MILIONE: a suite of computer programs for crystal structure solution of proteins. *J. Appl. Crystallogr., 40*(3), 609-613. http://dx.doi.org/10.1107/S0021889807010941

Checa, O., Diosa, J. E., Vargas, R. A., & Santamaria, J. (2009). Dielectric relaxation of $CsHSeO_4$ above room temperature. *Solid State Ionics, 180*(9-10), 673-676. http://dx.doi.org/10.1016/j.ssi.2009.03.010

Colomban, Ph., Pham-Thi, M., & Novak, A. (1986). Thermal history and phase transitions in the superionic protonic conductors $CsHSO_4$ and $CsHSeO_4$. *Solid State Ionics, 20*(2), 125-134. http://dx.doi.org/10.1016/0167-2738(86)90019-6

Farrugia, L. J. (1999). WinGX suite for small-molecule single-crystal crystallography. *J. Appl. Crystallogr., 32*(4), 837-838. http://dx.doi.org/10.1107/S0021889899006020

Foose, D., & Mitra, G. (1977). The crystal structure of cesium hydrogen selenate $CsHSeO_4$ (VI). *J. Inorg. Nucl. Chem., 39*(3), 553-554. http://dx.doi.org/10.1016/0022-1902(77)80082-1

Friesel, M., Baranowski, B., & Lundén, A. (1989). Pressure dependence of the transition to the proton conducting phase of $CsHSO_4$, $CsHSeO_4$ and $RbHSeO_4$ studied by differential scanning calorimetry. *Solid State Ionics, 35*(1-2), 85-89. http://dx.doi.org/10.1016/0167-2738(89)90016-7

Fukami, T., & Chen, R. H. (1999). Structural phase transitions and crystal structure for $Na_3D(SO_4)_2$ crystals at room temperature. *Phys. Stat. Sol. (b), 216*(2), 917-923. http://dx.doi.org/10.1002/(SICI)1521-3951(199912)216:2<917::AID-PSSB917>3.0.CO;2-2

Fukami, T., & Chen, R. H. (2003). Structural phase transition and crystal structure of a highly deuterated $(ND_4)_3D(SeO_4)_2$ crystal. *Phys. Stat. Sol. (a), 199*(3), 378-388. http://dx.doi.org/10.1002/pssa.200306664

Fukami, T., Miyazaki, J., Tomimura, T., & Chen, R. H. (2010a). Crystal structures and isotope effect on $Na_5H_3(SeO_4)_4 \cdot 2H_2O$ and $Na_5D_3(SeO_4)_4 \cdot 2D_2O$ crystals. *Cryst. Res. Technol., 45*(8), 856-862. http://dx.doi.org/10.1002/crat.201000116

Fukami, T., Tomimura, T., & Chen, R. H. (2010b). Geometric isotope effect and phase transition on $(NH_4)_2Co(SO_4)_2 \cdot 6H_2O$ Tutton salt. *J. Mater. Sci. Eng. Adv. Technol., 2*(2), 147-164. Retrieved from http://scientificadvances.org/journals6P5.htm

Ichikawa, M. (1978). The O-H vs O···O distance correlation, the geometric isotope effect in OHO bonds, and its application to symmetric bonds. *Acta Crystallogr. B, 34*(7), 2074-2080. http://dx.doi.org/10.1107/S0567740878007475

Ichikawa, M. (2000). Hydrogen-bond geometry and its isotope effect in crystals with OHO bonds - revisited. *J. Mol. Struct., 552*(1-3), 63-70. http://dx.doi.org/10.1016/S0022-2860(00)00465-8

Kamazawa, K., Harada, M., Ikedo, Y., Sugiyama, J., Tyagi, M., & Matsuo, Y. (2010). Long range proton diffusive motion of $CsHSO_4$ and $CsHSeO_4$: High energy resolution quasielastic neutron scattering of superprotonic conductors. *J. Phys. Soc. Japan, 79*, Suppl. A, 7-11. http://dx.doi.org/10.1143/JPSJS.79SA.12

Komukae, M., Tanaka, M., Osaka, T., Makita, Y., Kozawa, K., & Uchida, T. (1990). Hydrogen rearrangements in $CsHSeO_4$ accompanied with both the phase transition and domain-boundary-movement. *J. Phys. Soc. Japan, 59*(1), 197-206. http://dx.doi.org/10.1143/JPSJ.59.197

Lushnikov, S. G., Prokhoroval, S. D., Sinii, I. G., & Smolenskii, G. A. (1987). Elastic properties of the cesium deuterium selenate crystal in the monoclinic phase. *Sov. Phys. Solid State, 29*(2), 280-284.

Luspin, Y., Meneses, D. De S., & Simon, P. (2000). New Brillouin spectroscopy results in $CsHSeO_4$ between room temperature and the superionic transition. *Solid State Commun., 114*(7), 361-364. http://dx.doi.org/10.1016/S0038-1098(00)00066-1

Luspin, Y., Vaills, Y., & Hauret, G. (1995). Phase transitions in the superionic protonic conductor $CsHSeO_4$ investigated by Brillouin spectroscopy. *Solid State Ionics, 80*(3-4), 277-281. http://dx.doi.org/10.1016/0167-2738(95)00146-W

Ortiz, E., Tróchez, J. C., & Vargas, R. A. (2008). Phase behaviour of the solid proton conductor $CsHSeO_4$. *J. Phys. Condens. Matter, 20*(36), 365218. http://dx.doi.org/10.1088/0953-8984/20/36/365218

Ortiz, E., Vargas, R. A., & Mellander, B. E. (2006). Phase behaviour of the solid proton conductor $CsHSO_4$. *J. Phys. Condens. Matter, 18*(42), 9561-9573. http://dx.doi.org/10.1088/0953-8984/18/42/003

Pham-Thi, M., Colomban, Ph., Novak, A., & Blinc, R. (1985). Phase transitions in superionic protonic conductors $CsHSO_4$ and $CsHSeO_4$. *Solid State Commun., 55*(4), 265-270. http://dx.doi.org/10.1016/0038-1098(85)90605-2

Scheldrick, G. M. (1997). SHELXL-97, Program for Crystal Structure Refinement (University of Göttingen, Germany). Retrieved from http://shelx.uni-ac.gwdg.de/SHELX/

Yokota, S. (1982). Ferroelastic phase transition of $CsHSeO_4$. *J. Phys. Soc. Japan, 51*(6), 1884-1891. http://dx.doi.org/10.1143/JPSJ.51.1884

Yokota, S., Takanohashi, N., Osaka, T., & Makita, Y. (1982). Dielectric and thermal studies on new phase transition of $CsHSeO_4$. *J. Phys. Soc. Japan, 51*(1), 199-202. http://dx.doi.org/10.1143/JPSJ.51.199

Yoshida, Y., Hisada, K., Matsuo, Y., & Ikehata, S. (2008). NMR measurements on proton conductor $CsHSeO_4$ below T_c = 401K. *Solid State Ionics, 178*(37-38), 1869-1871. http://dx.doi.org/10.1016/j.ssi.2007.12.001

Yoshida, Y., Matsuo, Y., & Ikehata, S. (2005). ^{1}H-NMR and ^{77}Se-NMR in $CsHSeO_4$. *Solid State Ionics, 176*(31-34), 2457-2460. http://dx.doi.org/10.1016/j.ssi.2005.06.024